Design and fabrication of an embedded wire-grid nanograting*

Zhou Libing(周立兵)† and Zhu Wei(朱伟)

(Zhejiang Yangtze Delta Region Institute of Tsinghua University, Jiaxing 314200, China)

Abstract: An embedded wire-grid nanograting was designed and fabricated for using as a broadband polarizing beam splitter to reflect s-polarized light and transmit p-polarized light. A protected cladding layer of the same material as the grating's was deposited on the ridge, whereas the wire-grid is deposited in the grating trenches, which makes it more firm during application. High polarization extinction ratios of above 40 and 20 dB for transmission and reflection, respectively, with a broad wavelength range for the whole optical communication bandwidth (850 −1700 nm) and a wide angular tolerance ($> \pm 20^\circ$) are obtained by optimization of the designed structures, and the grating period is 200 nm.

Key words: polarizing beam splitter; wire-grid nanograting; extinction ratio
DOI: 10.1088/1674-4926/30/1/014006 **PACC:** 4225J; 4280F; 4280H

1. Introduction

The polarizing beam splitter (PBS) is a key element in photonic communication models, especially in devices such as switches, routers and isolators. These applications require that the PBS provides high extinction ratios, tolerates a wide incident angular range and a broad band of wavelength, and has a compact size for efficient packaging. Many types of PBSs have been applied in industry, such as natural crystal birefringence (e.g. Wollaston prisms), polarization selectivity of multilayer structures (e.g. PBS cubes) and fiber PBS. The Wollaston prism requires a large thickness to generate enough walk-off distance between the two orthogonal polarizations due to intrinsically small birefringence of the naturally anisotropic materials. An alternative design of Wollaston prism[1] reduces the thickness considerably by taking advantage of periodic multilayer slab structures that have form birefringence several times larger than that of natural birefringent materials. However, the fabrication of such a multilayer slab structure is a tedious and long process. PBS cubes are easier to fabricate, but they provide good extinction ratios only in a narrow angular bandwidth for a limited wavelength range[2]. Fiber PBS such as fused fiber PBS and photonic crystal fiber PBS have excellent polarization beam splitter character in the optical communication range but they are difficult to integrate with other optical elements[3,4].

In this paper, we introduce a new PBS device based on the unique properties of metal-wire nanogratings that consist of a series of fine parallel metallic lines usually coated on a glass substrate. These wire arrays polarize efficiently when the dimensions of the wires and spacings are small compared to the wavelength of the incident light. Light polarized parallel to the metal wires is reflected. Light polarized perpendicular to the wires is mainly transmitted. The most common explanation of the wire-grid polarizer is based on the restricted movement of electrons perpendicular to the metal wires[5]. If the incident wave is polarized along the wire direction, the conduction electrons are driven along the length of the wires with unrestricted movement. The coherently excited electrons generate a forward traveling wave as well as a backward traveling wave, with the forward traveling wave canceling the incident wave in the forward direction. The physical response of the wire grid is essentially the same as that of a thin metal sheet. As a result, the incident wave is totally reflected and nothing is transmitted in the forward direction. In contrast, if the incident wave is polarized perpendicular to the wire grid, and if the wire spacing is smaller than the wavelength, the Ewald–Oseen field generated by the electrons is not sufficiently strong to cancel the incoming field in the forward direction. Thus there is considerable transmission of the incident wave. The backward traveling wave is also much weaker, leading to a small reflectance. Thus most of the incident light is transmitted.

Although the concept of the wire grid polarizer has been around for a long time[5], there are still many limitations to its application in the optical communication region, the reasons being the challenging tasks of nano-scale grating fabrication, the poor adhesive and fragile properties of metal wire[6]. In our experience, we have developed a novel metal grid polarizer beam splitter using a nanofabrication technique, which imbedded the metal grating under a homogeneous material as the substrate. This kind of imbedded metal grid polarizer beam splitter can provide other beneficial optical properties and protect the polarizer. We shall use effective medium theory (EMT) for initial design and rigorous coupled wave analysis (RCWA) based software for optimization of the polarizing beam splitter. We shall also characterize them in terms of polarization efficiency for operation with waves of wide angular bandwidth and broad wavelength range. The results

* Project supported by the National Natural Science Foundation of China (No.60707017) and the Science and Technology Plan of Zhejiang Province, China (No.2006C1005).

† Corresponding author. Email: zlb100@163.com

Received 24 July 2008,revised manuscript received 8 September 2008

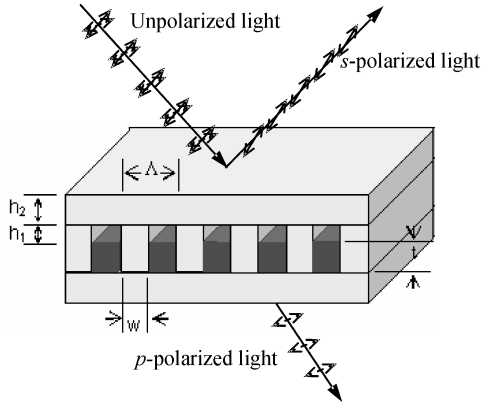

Fig.1. Schematic of an embedded metal wire nanograting. p-polarized light is transmitted and s-polarized light is reflected.

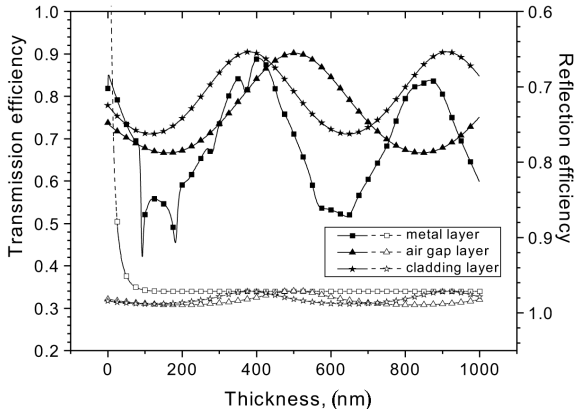

Fig.2. Polarization efficiency of s-polarized light reflection and p-polarized light transmission as functions of the thickness of each layer in the embedded metal-wire nanograting. The solid line means transmission and the dashed line means reflection. The incident wavelength was 1550 nm and the period of grating was 200 nm.

demonstrate extremely high polarization efficiency when the PBS is operated over ±20° incident angular bandwidth with wavelength ranging from 850 to 1700 nm.

2. Embedded metal-wire grating structure and design

Figure 1 shows a sketch of an embedded metal-wire nanograting. We use quartz wafer as the substrate because of its thermal stability, low absorption coefficients in the near infrared region (this results in a low insertion loss) and nearly the same refractive index as the upper cladding plasma-enhanced chemical vapor deposition (PECVD) SiO_2 layer. For operation of the form birefringent grating in the zero diffraction order we set the grating period equal to 0.2 μm (Λ = 200 nm). If period of the grating is sufficiently small compared with the wavelength, the whole structure behaves as if it was homogenous and uniaxially anisotropic, which are the attributes of form birefringence[7]. Orthogonally polarized light encounters different effective refractive indices because of the asymmetric grating structure. One polarization is parallel to the grating (s-polarized light) and the other is perpendicular to the grating (p-polarized light).

Consider a one-dimensional grating layer composed of

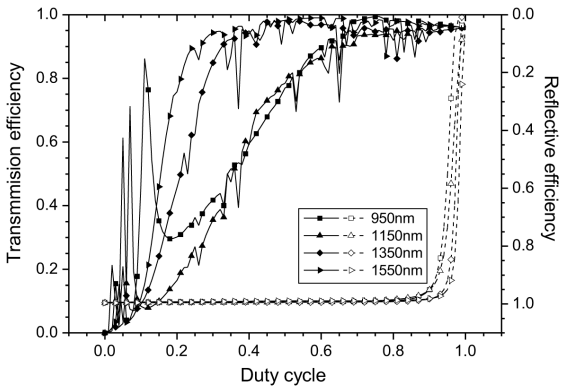

Fig.3. Polarization efficiency of s-polarized light reflection and p-polarized light transmission as functions of duty cycle (dc, w/Λ) at various wavelengths. The solid line means transmission and the dashed line means reflection. The period of grating was 200 nm. The thickness of metal, air-gap and upper cladding layers were 340, 480 and 380 nm, respectively.

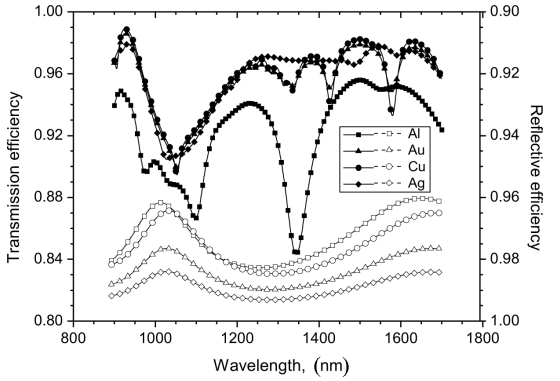

Fig.4. Polarization efficiency of s-polarized light reflection and p-polarized light transmission as functions of wavelength with various metal materials. The solid line means transmission and the dashed line means reflection. The period of grating was 200 nm. The thickness of metal, air-gap and upper cladding layers were 340, 480 and 380 nm, respectively, with 0.75 duty cycle.

two materials of refractive indices n_1 and n_2 with duty cycle f (f = width$_{(\text{material of n1})}$/period); the effective indices are given by[8]

$$n_{\parallel} = [fn_1^2 + (1-f)n_2^2]^{1/2}, \quad (1)$$

$$n_{\perp} = n_1 n_2 [fn_2^2 + (1-f)n_1^2]^{-1/2}. \quad (2)$$

Unpolarized light was incident upon the metallic grating. The first diffracted order, which was linearly polarized in the direction perpendicular to the grating array (p-polarized light), was designed to transmit through the nanograting. In contrast, the zeroth-diffracted order, which was linearly polarized in the direction parallel to the grating array (s-polarized light) was reflected[9].

The nanograting was designed to operate in the optical communication wave band (900–1700 nm). The diffraction efficiency was generally high in the long wavelength spectrum. For the short wavelength spectrum the diffraction efficiency decreased rapidly at resonance wavelength, as determined by

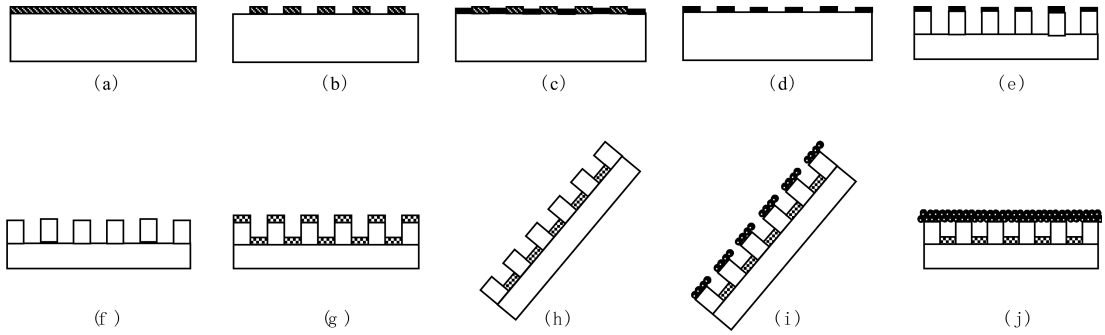

Fig.5. Steps in the fabrication of an embedded metal wire grating: (a) E-beam resist coating; (b) E-beam writing and development; (c) Cr film deposition; (d) E-beam resist lift-off; (e) Quartz substrate anisotropic etching; (f) Residual Cr stripped; (g) Ag film deposition; (h) Upper Ag film tilted etching; (i) Cladding layer tilted deposition; (j) Enhancing cladding layer thickness by deposition in a level position.

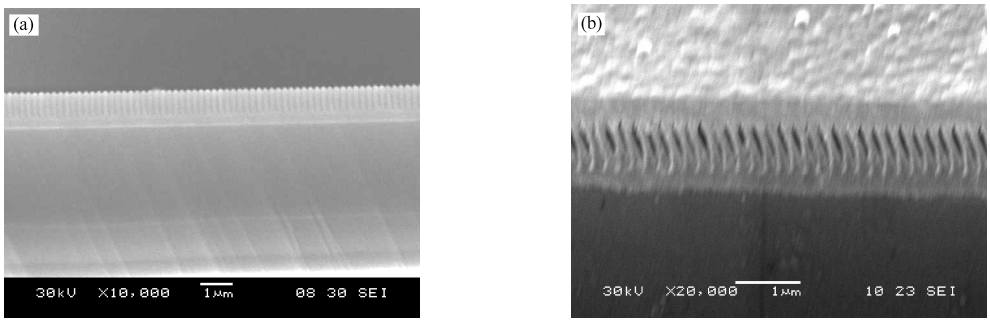

Fig.6. Scanning-electron microscope photographs of the grating: (a) 200 nm period nanograting with 0.75 duty cycle; (b) Embedded metal-wire nanograting.

$$\lambda = \Lambda(n_s \pm \sin\theta)/m, \tag{3}$$

where Λ is the period of the grating, n_s is the refractive index of the structure, and θ and m are the incident angle and the diffraction order, respectively. Low efficiency at short wavelengths results in narrowband spectrum applications. The limitation was overcome by optimizing the designed structure, including period (Λ), line width (w), line/layer depth or thickness (h_1, h_2 and t), properties of the grating material, and angle of incidence, etc. The theoretical efficiency of the diffracted orders of the embedded multilayer structures t was calculated with the commercial software Grating Solver, which uses rigorous coupled-wave analysis to yield the diffraction efficiencies and allows the complex refractive indices of the materials to be input[10].

Various layer thicknesses (shown in Fig.2), duty cycles (shown in Fig.3) and materials for the metal layer (shown in Fig.4) were simulated for transmission of p-polarized light and reflection of s-polarized light. It can be seen from Fig.2 that the variation of the thicknesses of the metal layer (t), the air-gap layer (h_1) and the upper cladding layer (h_2) have limited influence on the s-polarized light reflection efficiency, but the p-polarized light transmission efficiency changed periodically as the thickness increased. The polarization efficiency can be optimized flexibly by adjusting the depth of air gap between the upper cladding layer and metal wire and unlimited by the metal and substrate refractive indices, which is a more desirable characteristic than the compact sandwich structure[11]. Figure 3 reveals that a larger duty cycle (w/Λ) will result in greater bandwidth of high efficiency p-polarized light transmission, but the s-polarized light reflection efficiency would be depressed if the duty cycle is too high. In Fig.4, Ag has a better polarization performance than other metals, such as Al and Cu, and can be easily etched in Cl_2-based plasma. Other highly reflective metals, such as Au, can substitute for Ag without degrading polarization efficiency, but they are more expensive. Ag (t = 340 nm thick), air-gap (h_1 = 480 nm thick) and upper cladding SiO_2 layer (h_2 = 380 nm thick) with a 200 nm period, 0.75 duty cycle (w/Λ = 0.75) were eventually chosen because of their ease of use and high polarization efficiency in both transmission and reflection.

3. Fabrication

The fabrication steps are shown in Fig.5. We used E-beam lithography, plasma reactive ion etching, physical sputter deposition and PECVD process techniques to fabricate the embedded metal wire grating structure on quartz substrate. First, 0.2 μm thick poly-methyl-methacrylate (PMMA) was spin coated onto a quartz substrate to form a shadow mask. E-beam lithography was then used to define a high-resolution grating with a period of 0.2 μm and a duty cycle of 0.25. After development, a 0.1 μm thick Cr film was deposited sequentially. The PMMA pattern was then lifted off in acetone to yield the 0.75 duty cycle grating metal mask. Subsequently, CHF_3/O_2 plasma with a discharge voltage was used for anisotropic reactive ion etching of the quartz substrate to a depth of 820 nm. After the residual Cr mask was stripped off the substrate in a chemical etchant of $(NH_4)_2Ce(NO_3)_6(2)+HClO_4(1)+H_2O(9)$ mixed solution, a 340 nm Ag layer was deposited on the grating bottom and upper surface by physical sputter, and the grating upper Ag layer was then etched away

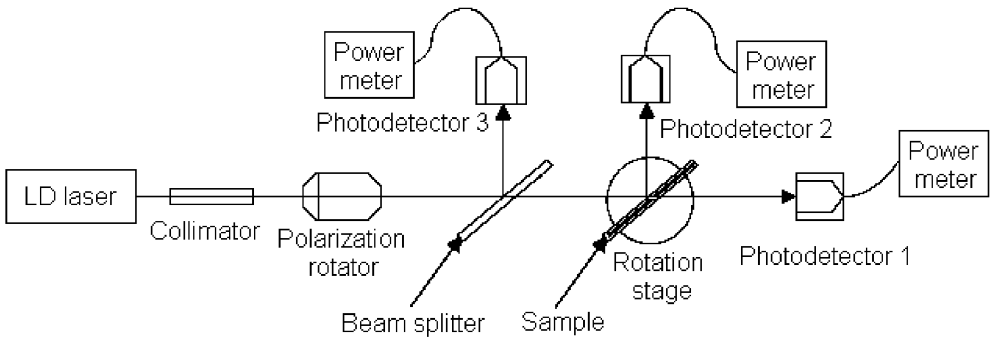

Fig.7. Schematic diagram of the experimental setup for the efficiency measurement of the fabricated embedded nanograting.

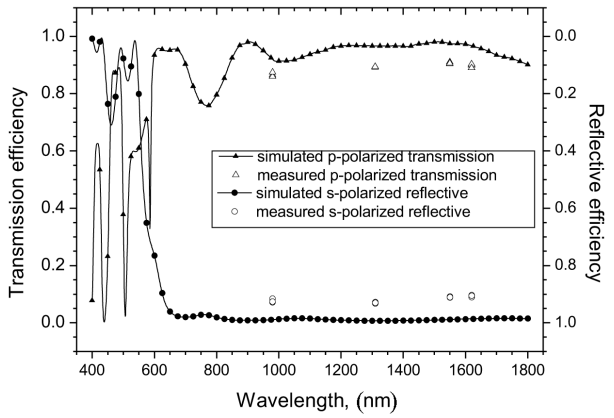

Fig.8. Comparison of experimental and simulated results of p-polarized light transmission and s-polarized light reflection efficiencies of the embedded metal-wire nanograting as functions of wavelength with incident angle 10 ° . The measured wavelength is 980, 1310, 1550 and 1620 nm, respectively.

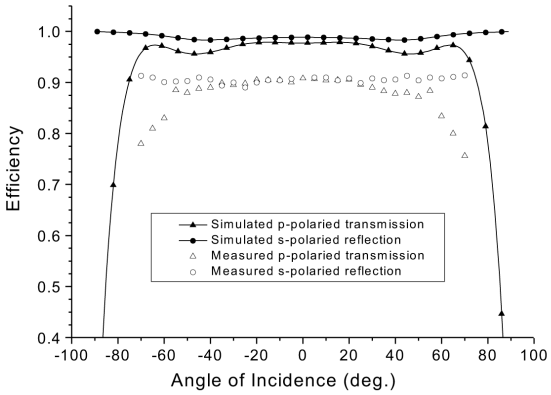

Fig. 9. Comparison of experimental and simulated results from the embedded metal-wire nanograting as functions of angle of incidence. Measurements at 1550 nm for both s-polarized and p-polarized light.

in Cl_2/Ar anisotropic plasma by titling the sample. The last process is to deposit a 380 nm thick SiO_2 layer on the grating surface by titling the sample in a PECVD chamber at first in the same way as in the Cl_2/Ar anisotropic plasma etch process and then depositing in a level position. The gratings fabricated in our experience are shown in Fig.6.

4. Polarizer characterization

The transmission and reflection of the fabricated embedded grating were measured with LD light sources at 980, 1310, 1550 and 1620 nm respectively. The measuring setup is shown schematically in Fig.7. The beam was focused onto the fabricated grating, and its input polarization was controlled by a polarization rotator. Three photodetectors were then used to measure the transmission, the reflection and the incident reference light simultaneously. The sample was mounted on a controllable rotation stage. The simulated and measured polarization properties of the embedded wire grating as functions of wavelength are shown in Fig.8. The incident angle of the light beam was 10 ° . It can be seen that this eventually chosen grating has high separation performance of the polarization beams at the optical communication wavelengths. The transmission efficiency has 0.3 dB variation (from a minimum loss of 0.09 dB at 1510 nm to a maximum loss of 0.38 dB at 990 nm) and the refection efficiency has 0.03 dB variety (from a minimum loss of 0.04 dB at 1320 nm to a maximum loss of 0.07 dB at 1050 nm) in the 850–1700 nm range. The simulated and measured efficiencies as functions of incident angle at 1550 nm wavelength are shown in Fig.9 (The reflection efficiency was measured for incident angles starting from ±5 °). It can be seen that the grating has a very broad range of incident light angle. No obvious variation in the transmission polarization efficiency is seen for a range of ±20 ° and only 0.1 dB fluctuation over a range of ±70 ° , from a minimum loss of 0.09 dB at ±15 ° to a maximum loss of 0.19 dB at ±46 ° . The reflective polarization efficiency has a maximum loss of 0.07 dB at ±42 ° over the whole range of incident angle. These properties give great angle tolerance to the device package. The difference in polarization efficiency between measured and simulated values could perhaps be attributed to the absorption of the materials and the effects of nonrectangular grating shape and structural dimension errors in fabrication. Reducing the grating period with a higher aspect ratio can reduce the effect of fabrication errors, which will be discussed in detail in subsequent work.

5. Conclusion

In conclusion, we have introduced a novel PBS device that is based on the characteristics of a metal wire binary nanograting. This PBS combines the form birefringence effect of a high spatial frequency grating with the high reflectance of metal wire embedded under a cladding layer. We use EMT

for initial design and RCWA-based software for optimization of the polarizing beam splitter. The results show that the embedded metal wire nanograting PBS not only provides a very high polarization efficiency for two orthogonal polarizations, but also can be operated with an optical signal of wide angular bandwidth (no obvious variation is seen in $\pm 20^\circ$ and only 0.1 dB variation in $\pm 70^\circ$) and broad spectral range (the transmission efficiency has 0.3 dB variation over the 850–1700 nm range; the reflection efficiency has 0.03 dB variation over the same range). The other advantage of this structure is that its performance can be optimized flexibly by adjusting the multilayer thickness unlimited by the metal and substrate refractive indices. The most extraordinary and excellent property of this embedded PBS is that it can be adhered with other optical elements optionally and can endure any physical impact during use as a result of its homogeneous upper cladding layer. These features make these devices desirable for use in optical communications as well as other polarization optics applications.

References

[1] Shiraishi K, Kawakami S. Spatial walk-off polarizer utilizing artificial anisotropic dielectrics. Opt Lett, 1990, 15(9): 516

[2] Pezzaniti J L, Chipman R A. Angular dependence of polarizing beam-splitter cubes. Appl Opt, 1994, 33(10): 1916

[3] Yataki M S, Payne D N. All-fiber polarizing beam splitter. Electron Lett, 1986, 13(15): 404

[4] Russell P, Knight J C, Birks T A, et al. Recent progress in photonics crystal fibers. OFC, 2000, 3: 98

[5] Hecht E. Optics. 3rd ed. New York: Addison-Wesley Longman, 1998

[6] Knop K. Reflection grating polarizer for the infrared. Opt Commun, 1978, 26(3): 281

[7] Yariv A, Yeh P. Optical waves in crystal. New York: Wiley, 1984

[8] Flory F, Escoubas L, Lazarides B. Artificial anisotropy and polarizing filters. Appl Opt, 2002, 41(16): 3332

[9] Soares L L, Cescato L. Metallized photoresist grating as a polarizing beam splitter. Appl Opt, 2001, 40(32): 5906

[10] Moharam M G, Gaylord T K. Diffraction analysis of dielectric surface-relief gratings. Optical Society of American, 1982, 72(10): 1385

[11] Yi D, Yan Y B, Liu H T, et al. Broadband polarizing beam splitter based on the form birefringence of a subwavelength grating in the quasi-static domain**.** Opt Lett, 2004, 29(7): 754